

Received 2 July 2018; revised 2 August 2018; accepted 3 August 2018. Date of publication 9 August 2018; date of current version 27 August 2018.
The review of this paper was arranged by Editor C.-M. Zetterling.

Digital Object Identifier 10.1109/JEDS.2018.2864720

High Breakdown-Voltage (>2200 V) AlGaN-Channel HEMTs With Ohmic/Schottky Hybrid Drains

WEIHANG ZHANG^{1b}, JINCHENG ZHANG^{1b}, MING XIAO^{1b}, LI ZHANG,
AND YUE HAO (Senior Member, IEEE)

State Key Discipline Laboratory of Wide Band-Gap Semiconductor Technology, School of Microelectronics, Xidian University, Xi'an 710071, China

CORRESPONDING AUTHOR: J. ZHANG (e-mail: jchzhang@xidian.edu.cn)

This work was supported by the National Key Research and Development Program of China under Grant 2016YFB0400105.

ABSTRACT In this paper, a high breakdown voltage of more than 2200 V in high-electron-mobility transistors (HEMTs) with AlGaN channel and a novel ohmic/Schottky-hybrid drain contact is achieved, which is the record breakdown voltage ever achieved on AlGaN-channel HEMTs. The fabricated device exhibits a high on/off ratio of 7×10^9 and a low subthreshold swing of 64 mV/decade, enabled by the AlGaN channel and wet treatment. Furthermore, it exhibits excellent high-temperature output characteristics and dynamic I_D - V_D characteristics. Even though both the AlGaN channel and the ohmic/Schottky-hybrid drain have certain impact on the on-state resistance because of the higher sheet resistance and drain contact resistance, these results indicate the significance and potential of AlGaN-channel HEMTs with a hybrid drain architecture in high-voltage applications.

INDEX TERMS AlGaN channel, ohmic/Schottky-hybrid drain, breakdown voltage, MOVPE.

I. INTRODUCTION

GaN-based high-electron-mobility transistors (HEMTs) have attracted great interest for power conversion applications due to their low loss and fast switching speeds [1], [2]. In order to extend these applications to the high voltage field, various material and device improvements have been reported to enhance breakdown voltage, using AlGaN channels [3], [4], AlGaN/GaN/AlGaN double-heterostructures [5], field plates [6], [7], or Schottky-sources/drains [8]. The AlGaN-channel HEMTs show great promise for high voltage applications due to an increased critical electric-field in AlGaN materials compared to GaN. However, it is extremely difficult to obtain AlGaN-channel HEMTs with high Al composition (>0.5) and excellent crystalline quality on a hetero-substrate owing to significant lattice and thermal mismatches between the AlGaN buffer layer and the hetero-substrate [9], [10]. Meanwhile, the breakdown voltage sees negligible improvement due to the poor crystalline quality that results from high Al composition. In addition, the reported breakdown field strengths of AlGaN channel HEMTs are much less than their expected critical

field strength. To the authors' best knowledge, currently no reports of a breakdown voltage exceeding 2000 V for AlGaN-channel HEMTs exists.

In this letter, we demonstrate a novel drain contact for AlGaN-channel HEMTs with an Al composition of 0.1 in the channel. This new drain contact can be obtained through only changing the design layout and without modifying (or increasing) device fabrication process steps. By combining the new drain contacts with the AlGaN channel, high breakdown voltages of more than 2200 V for HEMTs grown on a sapphire substrate are achieved. Furthermore, the technology is also anticipated to promote uniformity in the breakdown characteristics since the hybrid drain contacts feature much improved edge and surface metal morphology than the ohmic contacts merely formed through high-temperature annealing.

II. MATERIAL GROWTH AND DEVICE FABRICATION

The $\text{Al}_{0.3}\text{Ga}_{0.7}\text{N}/\text{Al}_{0.1}\text{Ga}_{0.9}\text{N}$ epitaxy in this work is grown on a two-inch c-plane sapphire substrate by a low-pressure metalorganic chemical-vapor-phase epitaxy system.

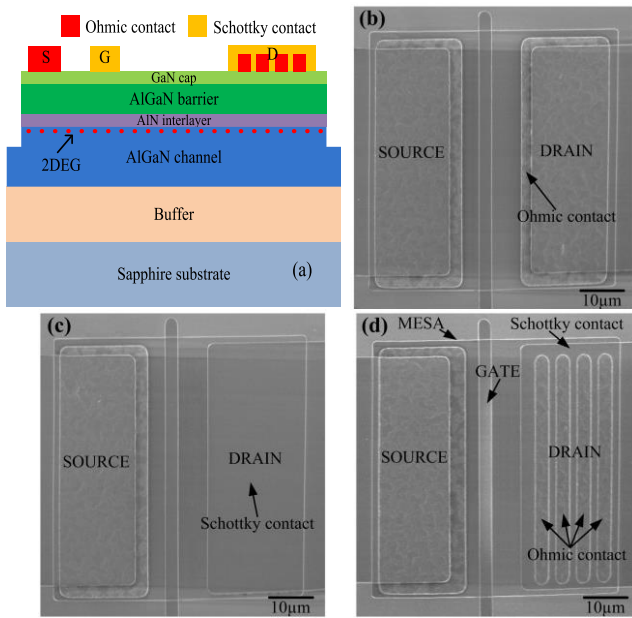


FIGURE 1. (a) Cross-sectional schematic diagram of the fabricated AlGaN-channel HEMT. (b)–(d) Top-view SEM images of the AlGaN-channel HEMTs with ohmic, Schottky, and ohmic/Schottky-hybrid drains, respectively.

Trimethylaluminum, trimethylgallium and ammonia (NH_3) are used as the precursors of Al, Ga and N, respectively. Hydrogen is used as the carrier gas. The substrates are annealed in NH_3 and H_2 mixed gas ambient for 10 min at 1050°C to remove the surface contamination before the epitaxial growth. The growth is initiated with a 180 nm high-temperature AlN nucleation (HT-AlN) layer grown at 1050°C , followed by a $1.1\ \mu\text{m}$ GaN buffer layer at 1000°C . In order to avoid the generation of parasitic channel and crack, a 300 nm linear-graded $\text{Al}_x\text{Ga}_{1-x}\text{N}$ transition layer from 0% to 10% Al content on top is grown at 1000°C , followed by a 200 nm $\text{Al}_{0.1}\text{Ga}_{0.9}\text{N}$ channel layer at 1000°C . Then, a 1 nm AlN interlayer, a 24 nm $\text{Al}_{0.3}\text{Ga}_{0.7}\text{N}$ barrier, and a 2 nm GaN cap layer are deposited. All the layers are unintentionally doped. At room temperature, the non-contact Hall measurements for the $\text{Al}_{0.3}\text{Ga}_{0.7}\text{N}/\text{Al}_{0.1}\text{Ga}_{0.9}\text{N}$ sample showed a sheet carrier density of $3.9 \times 10^{12}\ \text{cm}^{-2}$ and an electron mobility of $801\ \text{cm}^2\text{V}^{-1}\text{s}^{-1}$, respectively. The sheet resistance of the epitaxy is $2093\ \Omega/\square$. High resolution X-ray diffraction (XRD) and atomic force measurements (AFM) were performed to evaluate the device's crystalline quality and surface morphology, respectively. The (002) and (102) full-width at half-maxima (FWHM) for the $\text{Al}_{0.1}\text{Ga}_{0.9}\text{N}$ channel layer were 57 arcsec and 1292 arcsec, respectively. The surface roughness over an area of $20 \times 20\ \mu\text{m}^2$ in terms of root mean square for the $\text{Al}_{0.3}\text{Ga}_{0.7}\text{N}/\text{Al}_{0.1}\text{Ga}_{0.9}\text{N}$ heterostructure layer was 0.34 nm. For comparison, an $\text{Al}_{0.3}\text{Ga}_{0.7}\text{N}/\text{GaN}$ heterostructure which contains a 180 nm HT-AlN nucleation layer, a $1.6\ \mu\text{m}$ GaN buffer layer, a 1 nm AlN interlayer, a 24 nm $\text{Al}_{0.3}\text{Ga}_{0.7}\text{N}$ barrier, and a 2 nm GaN cap layer is also grown in the same

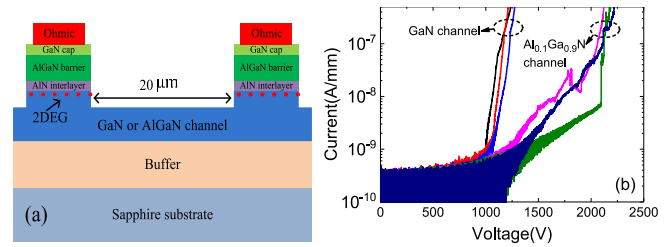


FIGURE 2. (a) Cross-sectional schematic of the fabricated isolation structures spurring from GaN and AlGaN channel epitaxy. (b) The channel breakdown characteristics of the GaN and AlGaN channel HEMTs.

conditions as that in the $\text{Al}_{0.3}\text{Ga}_{0.7}\text{N}/\text{Al}_{0.1}\text{Ga}_{0.9}\text{N}$ epitaxy. It exhibited a sheet carrier density of $9.2 \times 10^{12}\ \text{cm}^{-2}$ and an electron mobility of $2070\ \text{cm}^2\text{V}^{-1}\text{s}^{-1}$, which are higher than those of the $\text{Al}_{0.3}\text{Ga}_{0.7}\text{N}/\text{Al}_{0.1}\text{Ga}_{0.9}\text{N}$ heterostructure due to enhanced piezoelectric polarization and reduced alloy disorder scattering. The sheet resistance of the AlGaN/GaN heterostructure is $327\ \Omega/\square$. Figure 1(a) shows a cross-sectional schematic profile of the fabricated device. Device fabrication started with mesa isolation performed by BCl_3/Cl_2 inductively-coupled plasma (ICP) etching to a depth of 150 nm, followed by a tetramethylammonium hydroxide (TMAH) treatment with a 25% concentrated solution at 85°C for 10 min. Then, ohmic contact in the source and ohmic stripes in the drain were formed using Ti/Al/Ni/Au (22/140/55/45 nm) multilayer metals deposited by electron-beam evaporation, followed by a rapid thermal anneal at 840°C for 30 s in N_2 at atmospheric pressure. The four ohmic stripes in the drain have a length of $3\ \mu\text{m}$ and a spacing of $1.5\ \mu\text{m}$. The length of the Schottky metal between the gate-side drain edge and ohmic stripe is $3\ \mu\text{m}$. Finally, the gate electrodes and Schottky contacts covering the ohmic stripes in the drain terminal were fabricated by evaporation of a Ni/Au (45/200 nm) bilayer. Scanning electron microscopy (SEM) images of the AlGaN channel HEMTs with ohmic, Schottky, and ohmic/Schottky-hybrid drains are shown in Figs. 1(b), 1(c), and 1(d), respectively. The AlGaN-channel HEMTs have a gate length $L_G = 3\ \mu\text{m}$, a gate width $W_G = 50\ \mu\text{m}$, a source-gate distance $L_{SG} = 3\ \mu\text{m}$, and a gate-drain distance $L_{GD} = 6 - 22\ \mu\text{m}$.

III. MEASUREMENTS AND RESULTS

The isolation structures in Fig. 2(a) were fabricated to evaluate the buffer breakdown characteristics of the GaN and AlGaN channel HEMTs. We can see from Fig. 2(b) that the breakdown voltage for the GaN channel reaches 1200 V with $20\ \mu\text{m}$ of isolation spacing. The breakdown voltage for the $\text{Al}_{0.1}\text{Ga}_{0.9}\text{N}$ channel with the same isolation spacing is more than 2000 V, which is 1.6 times that of the GaN channel. The higher breakdown voltage from the $\text{Al}_{0.1}\text{Ga}_{0.9}\text{N}$ channel results not only because of the higher breakdown strength of the AlGaN material itself, but also due to AlGaN epitaxy with good crystalline quality.

From Fig. 3(a), it is evident that the GaN-channel HEMTs have a larger saturation current density of $481\ \text{mA}/\text{mm}$

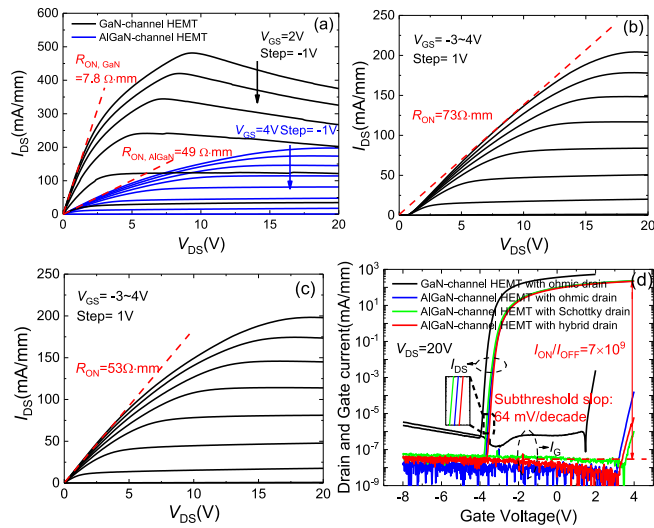


FIGURE 3. (a) I_{DS} - V_{DS} measurement curves for the GaN and AlGaN channel HEMTs. Output characteristics of the AlGaN-channel HEMTs with (b) Schottky drain and (c) ohmic/Schottky-hybrid drain with $L_{GD} = 6\ \mu\text{m}$. (d) Drain and gate current vs. gate voltage for the $\text{Al}_{0.3}\text{Ga}_{0.7}\text{N}/\text{GaN}$ and $\text{Al}_{0.3}\text{Ga}_{0.7}\text{N}/\text{Al}_{0.1}\text{Ga}_{0.9}\text{N}$ HEMT with different drain contacts for $V_{DS} = 20\ \text{V}$.

than that of 198 mA/mm for AlGaN-channel HEMTs mainly due to their lower sheet resistance. To follow-up on these experiments, the saturation current density of the AlGaN-channel HEMTs can be improved by increasing the Al component of the barrier layer. The drain current collapse in GaN-channel HEMTs in Fig. 3(a) is related to self-heating due to the poor thermal conductivity of sapphire substrate. Figures 3(b) and 3(c) show the output characteristics of the $\text{Al}_{0.3}\text{Ga}_{0.7}\text{N}/\text{Al}_{0.1}\text{Ga}_{0.9}\text{N}$ HEMTs with the Schottky and ohmic/Schottky-hybrid drains, respectively. The ohmic/Schottky-hybrid has a certain impact on the on-state resistance of the $\text{Al}_{0.3}\text{Ga}_{0.7}\text{N}/\text{Al}_{0.1}\text{Ga}_{0.9}\text{N}$ HEMTs; in comparison, the on-state resistance of the Schottky drain is higher, resulting from a higher contact resistance. Figure 3(d) demonstrates the transfer and gate-leakage characteristics for the GaN and AlGaN channel HEMTs with different drain contacts. Changing the drain contact for the AlGaN-channel HEMT has negligible impact on its transfer characteristics. However, the AlGaN-channel HEMTs have a lower reverse gate-leakage current than their GaN counterparts because AlGaN has deeper energy-level traps than GaN [11]. Therefore, the off-state currents for the AlGaN-channel HEMTs are lower than for GaN. As is well known, the gate-leakage current consists of surface, bulk, and mesa edge leakages [12]. This work employed a tetramethylammonium hydroxide (TMAH) treatment with a 25% concentrated solution at 85°C for 10 min to eliminate etching damage and to smoothen the recessed surface after the mesa isolation process [13]. Finally, the process obtained an I_{ON}/I_{OFF} ratio of 7×10^9 and subthreshold swing of 64 mV/decade for the AlGaN-channel HEMTs.

Figure 4 (a) and (b) show I_{DS} - V_{DS} measurement curves as a function of temperature for GaN-channel HEMT

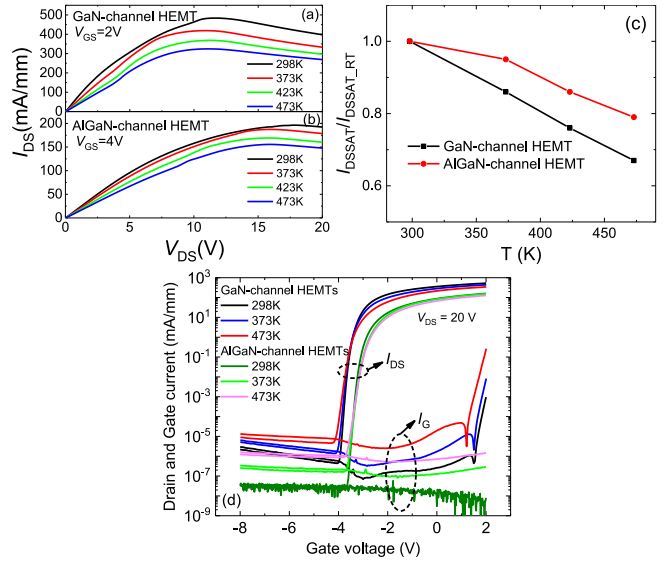


FIGURE 4. I_{DS} - V_{DS} measurement curves as a function of temperature for (a) GaN-channel HEMT and (b) AlGaN-channel HEMT with hybrid drain contacts and $L_{GD} = 6\ \mu\text{m}$. (c) Normalized drain current as a function of temperature for GaN-channel HEMT and for AlGaN-channel HEMT. (d) Transfer and gate leakage characteristics as a function of temperature for GaN-channel and AlGaN-channel HEMTs with hybrid drain.

and AlGaN-channel HEMT with hybrid drain contacts, respectively. The drain currents decrease with the increasing temperature for both devices. However, it can be seen from the temperature dependence of normalized drain current for both devices in Fig. 4 (c) that AlGaN-channel HEMT exhibits better output characteristics at elevated temperatures compared with GaN-channel HEMT, which is mainly because of the weaker mobility degradation for the AlGaN-channel heterostructure at elevated temperatures [14]. The threshold voltage is defined as V_G at $I_D = 1\ \mu\text{A}/\text{mm}$. As shown in Fig. 4(d), the AlGaN-channel HEMTs exhibit a smaller threshold voltage shift of 70 mV than that of 100 mV for GaN-channel HEMTs as the measurement temperature rises from 298 K to 473 K. Moreover, the gate leakage current increases with increasing temperature for both devices due to the surface-related traps and temperature assisted tunneling mechanism [15].

The pulsed I_{DS} - V_{DS} characteristics of the GaN-channel HEMT with ohmic drain and AlGaN-channel HEMTs with ohmic drain and hybrid drain are showed in Fig. 5(a), 5(b), and 5(c), respectively. Compared with GaN-channel HEMTs, it can be clearly seen that AlGaN-channel HEMTs exhibit negligible drain saturation current collapses because of the lower trap density in AlGaN-channel HEMTs [11]. Meanwhile, comparing Figs. 5(b) and 5(c) shows that the hybrid drain has no impact on the dynamic characteristics of the devices.

The off-state breakdown characteristics of the $\text{Al}_{0.3}\text{Ga}_{0.7}\text{N}/\text{GaN}$ and $\text{Al}_{0.3}\text{Ga}_{0.7}\text{N}/\text{Al}_{0.1}\text{Ga}_{0.9}\text{N}$ HEMTs with different drain contacts and gate-drain spacings are shown in Fig. 6. The breakdown voltage is defined by the criteria of leakage current reaching $0.5\ \mu\text{A}/\text{mm}$.

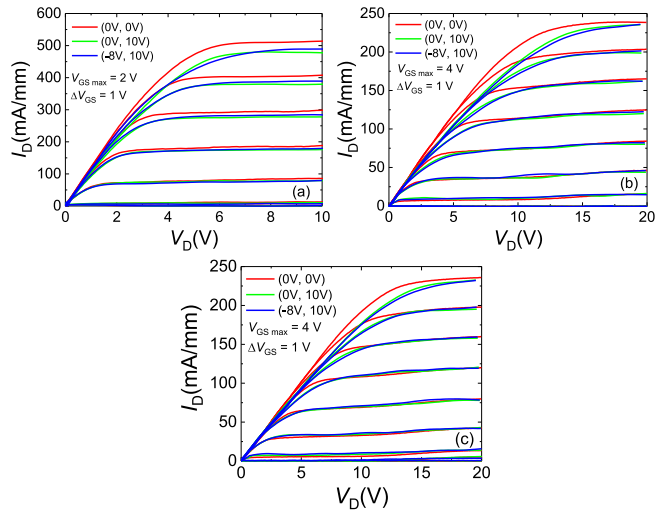


FIGURE 5. Pulsed I_{DS} - V_{DS} measurements for (a) GaN-channel HEMT, (b) AlGaN-channel HEMT with ohmic drain contacts and (c) AlGaN-channel HEMT with hybrid drain contact with $L_{GD} = 6 \mu\text{m}$. Quiescent points: ($V_{GS0} = 0 \text{ V}$, $V_{DS0} = 0 \text{ V}$), ($V_{GS0} = 0 \text{ V}$, $V_{DS0} = 10 \text{ V}$), ($V_{GS0} = -8 \text{ V}$, $V_{DS0} = 10 \text{ V}$). The pulse width and period of $1 \mu\text{s}$ and 10 ms were used, respectively.

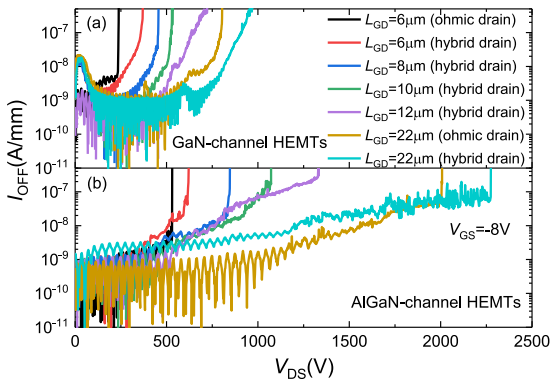


FIGURE 6. The breakdown measurement curves for $\text{Al}_{0.3}\text{Ga}_{0.7}\text{N}/\text{GaN}$ and $\text{Al}_{0.3}\text{Ga}_{0.7}\text{N}/\text{Al}_{0.1}\text{Ga}_{0.9}\text{N}$ HEMTs with different drain contacts and gate-drain spacings.

As shown in Fig. 6, the breakdown voltage of the $\text{Al}_{0.3}\text{Ga}_{0.7}\text{N}/\text{Al}_{0.1}\text{Ga}_{0.9}\text{N}$ HEMT with an ohmic contact and L_{GD} of $6 \mu\text{m}$ is much greater than that of the $\text{Al}_{0.3}\text{Ga}_{0.7}\text{N}/\text{GaN}$ HEMT. It is known, that carbon incorporation (acts as compensation dopant) during GaN growth is less than for AlGaN growth [16]. The reduced C-concentration of the GaN channel leaves it slightly n-type (typically due to O_2 or Si incorporation during MOCVD) and thus reduces the channel blocking significantly below its intrinsic limits. The breakdown voltage of the $\text{Al}_{0.3}\text{Ga}_{0.7}\text{N}/\text{Al}_{0.1}\text{Ga}_{0.9}\text{N}$ HEMT with a hybrid contact and L_{GD} of $6 \mu\text{m}$ is greater than that with only the ohmic contact, attributable to better edge and surface metal morphology [8]. The breakdown voltages of the $\text{Al}_{0.3}\text{Ga}_{0.7}\text{N}/\text{Al}_{0.1}\text{Ga}_{0.9}\text{N}$ HEMTs with the hybrid contact and $L_{GD} = 8, 10, 12,$ and $22 \mu\text{m}$ reach 846, 1072, 1336,

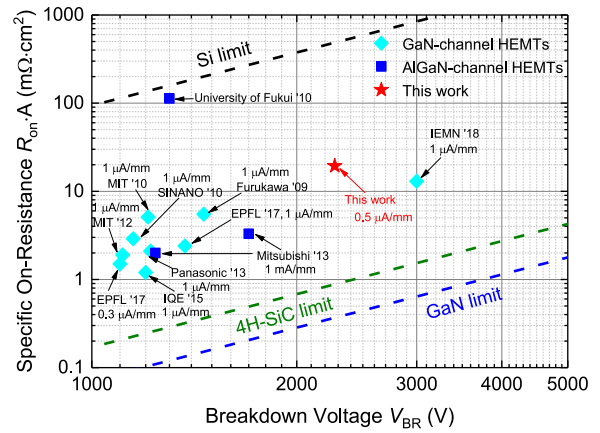


FIGURE 7. Benchmark of AlGaN-channel HEMTs and GaN-channel HEMTs with breakdown voltage defined at $I_{OFF} = 1 \mu\text{A}/\text{mm}$.

and 2274 V, respectively. These results are benchmarked against the GaN HEMTs reported by other groups (Fig. 7). A strict criterion of $1 \mu\text{A}/\text{mm}$ was adopted in Fig. 7 for a low off-state dissipated power. Noticeably, the device in this work still demonstrates a high specific on-resistance. The higher Al composition in the barrier or another heterostructure with a thin GaN layer inserted between the AlGaN channel and AlN interlayer will be implemented to reduce the specific on-resistance in our subsequent study. Even so, these results still make the AlGaN-channel HEMTs with hybrid contacts very promising for application in power devices requiring 1200 V or even more.

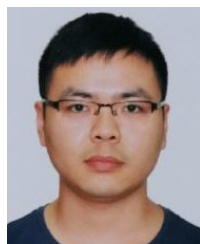
IV. CONCLUSION

We have demonstrated a combination of AlGaN channels and new ohmic/Schottky-hybrid drain contacts to improve the breakdown voltage of transistor devices, and a breakdown voltage of more than 2200 V for devices with $L_{GD} = 22 \mu\text{m}$ was achieved. This is the first report showing a breakdown voltage exceeding 2000 V for an AlGaN-channel HEMT. In addition, by using the AlGaN buffer and a wet treatment, a low subthreshold swing of 64 mV/decade and a high on/off ratio of 7×10^9 were obtained. The output characteristics at elevated temperatures and the dynamic characteristics of the devices were also improved. These improved results demonstrate important potential of this fabricated structure in the future for power switching applications requiring breakdown voltages more than 1200 V.

REFERENCES

- [1] Y. Wu, M. Jacob-Mitos, M. L. Moore, and S. Heikman, "A 97.8% efficient GaN HEMT boost converter with 300-W output power at 1 MHz," *IEEE Electron Device Lett.*, vol. 29, no. 8, pp. 824–826, Aug. 2008, doi: [10.1109/LED.2008.2000921](https://doi.org/10.1109/LED.2008.2000921).
- [2] W. Saito *et al.*, "A 120-W boost converter operation using a high-voltage GaN-HEMT," *IEEE Electron Device Lett.*, vol. 29, no. 1, pp. 8–10, Jan. 2008, doi: [10.1109/LED.2007.910796](https://doi.org/10.1109/LED.2007.910796).
- [3] T. Nanjo *et al.*, "AlGaN channel HEMT with extremely high breakdown voltage," *IEEE Trans. Electron Devices*, vol. 60, no. 3, pp. 1046–1053, Mar. 2013, doi: [10.1109/TED.2012.2233742](https://doi.org/10.1109/TED.2012.2233742).

- [4] T. Nanjo *et al.*, "First operation of AlGa_N channel high electron mobility transistors," *Appl. Phys. Exp.*, vol. 1, no. 1, pp. 1–3, Jan. 2008, doi: [10.1063/1.2949087](https://doi.org/10.1063/1.2949087).
- [5] E. Bahat-Treidel *et al.*, "AlGa_N/Ga_N/AlGa_N DH-HEMTs breakdown voltage enhancement using multiple grating field plates (MGFPs)," *IEEE Trans. Electron Devices*, vol. 57, no. 6, pp. 1208–1216, Jun. 2010, doi: [10.1109/LED.2010.2045705](https://doi.org/10.1109/LED.2010.2045705).
- [6] Y. Dora *et al.*, "High breakdown voltage achieved on AlGa_N/Ga_N HEMTs with integrated slant field plates," *IEEE Electron Device Lett.*, vol. 27, no. 9, pp. 713–715, Sep. 2006, doi: [10.1109/LED.2006.881020](https://doi.org/10.1109/LED.2006.881020).
- [7] S. Karmalkar and U. K. Mishra, "Enhancement of breakdown voltage in AlGa_N/Ga_N high electron mobility transistors using a field plate," *IEEE Trans. Electron Devices*, vol. 48, no. 8, pp. 1515–1521, Aug. 2001, doi: [10.1109/16.936500](https://doi.org/10.1109/16.936500).
- [8] Q. Zhou *et al.*, "Schottky-contact technology in InAlN/GaN HEMTs for breakdown voltage improvement," *IEEE Trans. Electron Devices*, vol. 60, no. 3, pp. 1075–1081, Mar. 2013, doi: [10.1109/TEDE.2013.2241439](https://doi.org/10.1109/TEDE.2013.2241439).
- [9] A. G. Baca *et al.*, "An AlN/Al_{0.85}Ga_{0.15}N high electron mobility transistor," *Appl. Phys. Lett.*, vol. 109, no. 3, pp. 1–4, Jul. 2016, doi: [10.1063/1.4959179](https://doi.org/10.1063/1.4959179).
- [10] S. Muhtadi *et al.*, "High electron mobility transistors with Al_{0.65}Ga_{0.35}N channel layers on thick AlN/sapphire templates," *IEEE Electron Device Lett.*, vol. 38, no. 7, pp. 914–917, Jul. 2017, doi: [10.1109/LED.2017.2701651](https://doi.org/10.1109/LED.2017.2701651).
- [11] S. Zhao *et al.*, "Trap states in AlGa_N channel high-electron-mobility transistors," *Appl. Phys. Lett.*, vol. 103, no. 21, pp. 1–4, Nov. 2013, doi: [10.1063/1.4832482](https://doi.org/10.1063/1.4832482).
- [12] W. S. Tan *et al.*, "Surface leakage currents in SiN_x passivated AlGa_N/Ga_N HFETs," *IEEE Electron Device Lett.*, vol. 27, no. 1, pp. 1–3, Jan. 2006, doi: [10.1109/LED.2005.860383](https://doi.org/10.1109/LED.2005.860383).
- [13] K. Kim *et al.*, "Effect of TMAH treatment on device performance of normally off Al₂O₃/Ga_N MOSFET," *IEEE Electron Device Lett.*, vol. 32, no. 10, pp. 1376–1378, Oct. 2011, doi: [10.1109/LED.2011.2163293](https://doi.org/10.1109/LED.2011.2163293).
- [14] X. Li *et al.*, "AlGa_N channel MIS-HEMTs with a very high breakdown electric field and excellent high-temperature performance," *IEICE Electron. Exp.*, vol. 12, no. 20, Oct. 2015, Art. no. 20150694, doi: [10.1587/elex.12.20150694](https://doi.org/10.1587/elex.12.20150694).
- [15] S. Arulkumaran, T. Egawa, H. Ishikawa, and T. Jimbo, "Temperature dependence of gate-leakage current in AlGa_N/Ga_N high-electron mobility transistors," *Appl. Phys. Lett.*, vol. 82, no. 18, pp. 3110–3112, Mar. 2003, doi: [10.1063/1.1571655](https://doi.org/10.1063/1.1571655).
- [16] G. Parish, S. Keller, S. P. Denbaars, and U. K. Mishra, "SIMS investigations into the effect of growth conditions on residual impurity and silicon incorporation in Ga_N and Al_xGa_{1-x}N," *J. Electron. Mater.*, vol. 29, no. 1, pp. 15–20, Jan. 2000, doi: [10.1007/s11664-000-0087-3](https://doi.org/10.1007/s11664-000-0087-3).



WEIHANG ZHANG received the B.S. degree in electronic science and technology from Xidian University, Xi'an, China, in 2013, where he is currently pursuing the Ph.D. degree with the School of Microelectronics.

His current research interests include the fabrication, characterization, and reliability analysis of GaN-based power devices.



JINCHENG ZHANG received the M.S. and Ph.D. degrees from Xidian University, Xi'an, China, in 2001 and 2004, respectively, where he is currently a Professor. His current research interests include wide gap-band semiconductor GaN and diamond materials and devices.

MING XIAO received the M.S. degree and the Ph.D. degree in microelectronics and solid-state electronics from Xidian University, Xi'an, China, in 2015 and 2018, respectively.

His current research interests include GaN-based power devices.



LI ZHANG received the B.S. degree and M.S. degree in microelectronics and solid-state electronics from Xidian University, Xi'an, China, in 2015 and 2018, respectively.

His current research interests include GaN-based power devices.



YUE HAO (SM'92) is currently a Professor of microelectronics and solid state electronics with Xidian University, Xi'an, China. His current research interests include wide gap-band materials and devices, advanced CMOS devices and technology, semiconductor device reliability physics, and failure mechanism and organic electronics.

He is a member of the Chinese Academy of Science.